Fast Hybrid Methods for Conformal Antenna, Array and Frequency Selective Surface Simulations

J. L. Volakis, E. Topsakal,Y. Erdemli, T. F. Eibert, L. Andersen and D. Filipovic
Radiation Laboratory, Electrical Engineering and Computer Science Department
The University of Michigan, 1301 Beal Ave, Ann Arbor, MI 48109-2122, USA

1. Introduction

This paper is on the use and development of fast algorithms for infinite and finite periodic array/frequency selective surface modeling (scattering, radiation and transmission) in the contest of hybrid methods. As is often the case, the highly adaptable (in terms of geometry and material characterization) finite element method is used for modeling the multilayer dielectric region of the array whereas the boundary integral serves as a means for truncating the finite element mesh. This formulations leads to hybrid matrix systems with the periodic boundary conditions placed along the periphery of the unit cell. The boundary integral submatrix typically consumes most of the CPU requirements and therefore much effort has been devoted over the years to speed up its calculations in the context of iterative solvers. In this paper we will address particular challenges in modeling

- Broadband antennas (such as spirals) containing small features across their aperture
- Large arrays (patches, slots, LTSAs) on multilayer substrates
- Frequency selective surfaces in multilayered environments
- Large finite arrays on curved platforms
- Large tapered radomes

Both infinite and finite arrays will be considered and comparisons will be given with traditional moment method implementations in terms of accuracy, memory and speed-up.

Three fast methods will be examined for infinite and finite array applications, and various applications of narrowband and broadband antennas will be considered. Emphasis will be particularly given on the use of multiresolution elements for volume and surface modeling. These elements are used in conjunction with adaptive error control, and we will show that inclusion of just a few of these elements will result in dramatic accuracy improvements for impedance calculations.

2. Applications

Perhaps, the best way to demonstrate advances in antenna and array modeling is consider some applications. Due to the limited space available for this paper, three of the five applications mentioned above will be considered.

2.1 Input Impedance of Linearly Tapered Slot Antenna (LTSA)

LTSAs are particularly attractive because of their broadband characteristics (5:1 bandwidth is typical) and low cross polarization properties. Analysis and design using finite element-boundary integral methods permits modeling of dielectric loading and feed details. However, using one mesh for accurate simulation over the 5:1 bandwidth will lead to inaccurate results. Also, requirements for good feed modeling implies fine meshing of the feed detail, a situation which may lead to inefficient discretization. A way to overcome the need for remeshing and

excessive gridding around the feed is to employ multiresolution or hierachical elements for expanding the field coupled with error indicators. In this context, a coarse mesh is constructed and used for an initial calculation of the fields within the antenna region. The field error (usually, the average discontinuity of the flux density across the elements) within each element or groups of them is then evaluated and used to adaptively increase the multiresolution order within each element. Of importance is that this type of p-adaptivity is done automatically without a need for re-meshing once we pre-specify the percentage of elements to be adaptively changed. To observe the significance of p-adaptivity, lets consider the LTSA shown in Figure 1. This LTSA is operating at 10GHz and is fed by a probe at the end of the narrow end of the LTSA. For numerical simulation, the LTSA is placed in a rectangular cavity whose side walls are 1.65cm all around the antenna surface and edges. Also, to simulate a free space environments (in as much as possible), the cavity walls are coated with a 0.15cm absorber having relative permittivity and permeability of 1-j2.7. Using a coarse mesh, the resulting volume was discretized using 44,370 elements, 91,269 faces and 55,621 edges (a dense mesh to recover the actual input impedance would be more than 3 times larger).

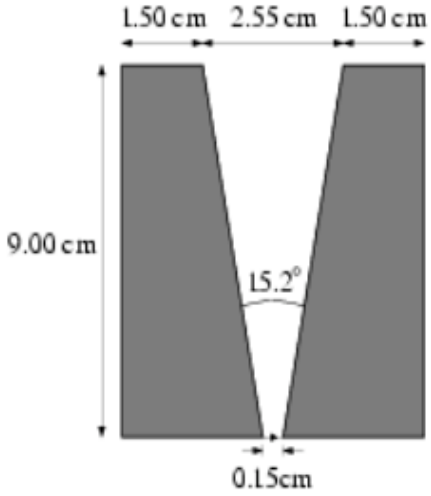

Figure 1a. Geometry of LTSA

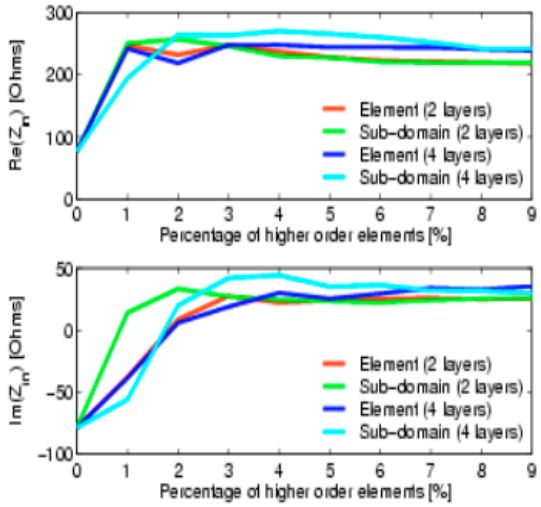

Figure 1b. Input impedance as a function of the % of higher order elements used in the mesh.

To apply p-adaptivity, we considered 4 ways for computing the field error. These are listed in Figure 1b and refer to the way used for grouping the elements. As seen, irrespective of the grouping for error computation, the conclusion is that only 2-3% of higher order elements (in this case 1.5 tangential vector finite elements-TVFE were used) are needed to recover the correct input impedance. This is certainly a much more efficient approach than blindly increasing the mesh size by a factor of three to four..

2.2 Frequency Selective Surface(FSS) Modeling with Non-Commensurate Layers as Ground Planes for Reconfigurable Arrays

An important aspect of hybrid finite element methods is the capability to simulate and design structures which are very complex in geometry and incorporate a variety of materials. A multilayer FSS or a frequency selective volume (commonly referred to as bandgap geometries) in the presence of antennas is one such structure. For the specific application of interest, the goal is to design a FSS to serve as a ground plane for conformal installation of broadband antennas. In this case, the FSS is designed to reflect a wave that is in phase with the direct wave radiated by the antenna towards the horizon (see Figure 2a). For practical

purposes, our FSS design objectives are **Magnitude :** $0.4 < |\Gamma| < 1.0$, **Phase :** $-50^o < \angle\Gamma < 50^o$, where Γ denotes the FSS reflection coefficient, over a 0.8-2.4GHz bandwidth. It is noted that ideally, we desire $|\Gamma| = 1$. However, such a requirement on Γ would theoretically preclude the possibility of limiting the phase variation to within acceptable bounds (in this case, a variation of $\pm 50^o$ in phase is acceptable). The chosen design objectives for Γ takes into consideration these theoretical issues. It was necessary to use resistive loading within the volume and preferably on the same surface of the FSS to introduce the loss (see Figure 2b). It is further important to note that the FSS must be non-commensurate to achieve the required performance over the 3:1 bandwidth. Modeling of such an FSS structure required a generalization in the application of the periodic boundary

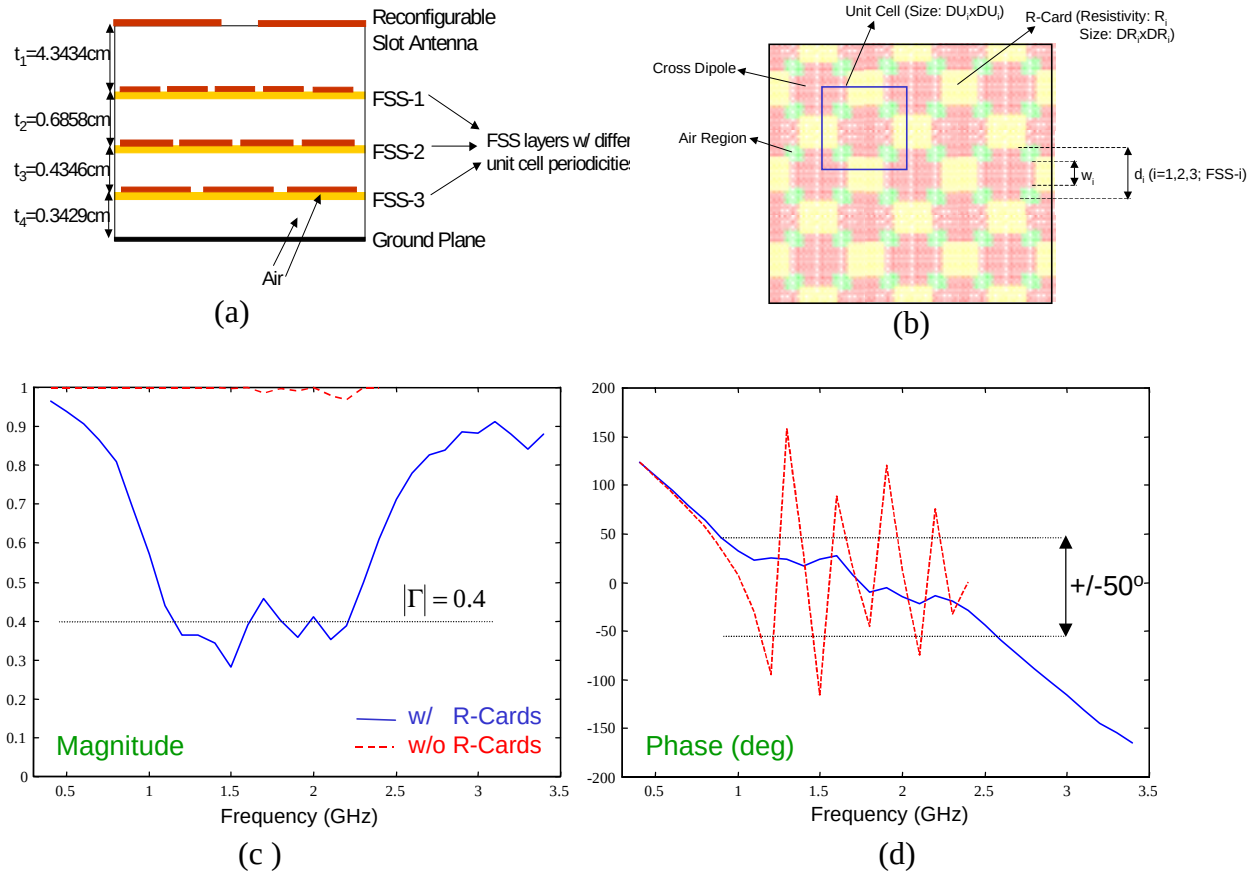

Figure 2. (a) cross section of the FSS structure; (b) layout of the FSS surface with possible resistive loading; (c) mag. of Γ for the designed non-commensurate FSS structure; (d) phase of G for the designed FSS.

conditions. The performance for a 3-layer FSS design is given in Figures 2c and 2d. The actual FSS design had periodicities of 10cm, 12cm, 16cm for each of the layers, and consisted of crossed dipole elements of lengths 5.89cm, 7.56cm and 10.7762cm for each of the corresponding FSS layers. More details will be given at the presentation, including data for the reconfigurable (using MEMS) antenna performance

2.3 Wideband Conformal Cavity-Backed Slot Spiral Analysis

The simulation of domains which incorporate small but important geometrical features is well known to be rather challenging. Nevertheless, this is the typical case with antennas as is the case with broadband spirals and more specifically with slot spirals. In this case the radiating slot is extremely narrow (a few mils), but the cavity (see Figure 3) is comparatively large.

Thus, a straightforward discretization of the domain will lead to rather large numerical systems. To avoid this extreme situation, we instead employed mixed elements, and for our case we used bricks for modeling the slot region and prisms elsewhere. This approach also avoids the problematic introduction of diagonal edges across the slot which will lead to ill conditioned systems since such edges are associated with vanishing fields. The development of such a robust computational tool proved important for the design of very thin (less than 2") broadband antennas having a 100:1 bandwidth (from HF frequencies up to 3GHz). Also, by using this computational tool we were able to design terminations for truncating the slot spiral arms and thus enhance its bandwidth and improve its axial ratio. Specifically, let us consider the slot spiral configurations in Figure 3 whose dimensions are max diameter d=14.57cm; cavity depth D=1.27cm; substrate thickness t=0.0508cm, ε_{sub}=3.38,-j0.009; slot width w=0.0782cm. The slot was terminated using a set of 60 chip resistors which varied from 1430Ω to 158Ω. Further, to suppress cavity resonances, vertical resistors were placed at the cavity rim (see Figure 3--top right). A total of 194 resistors, each having a value of R=150 Ω (unoptimized) were employed. The computed gain from 0.2-4GHz is give in the Figure and is compared to measurements. We observe that the agreement between measurements and calculation is rather remarkable over this 20:1 bandwidth. Even the more sensitive axial ratio parameter is in good agreement with measurements.

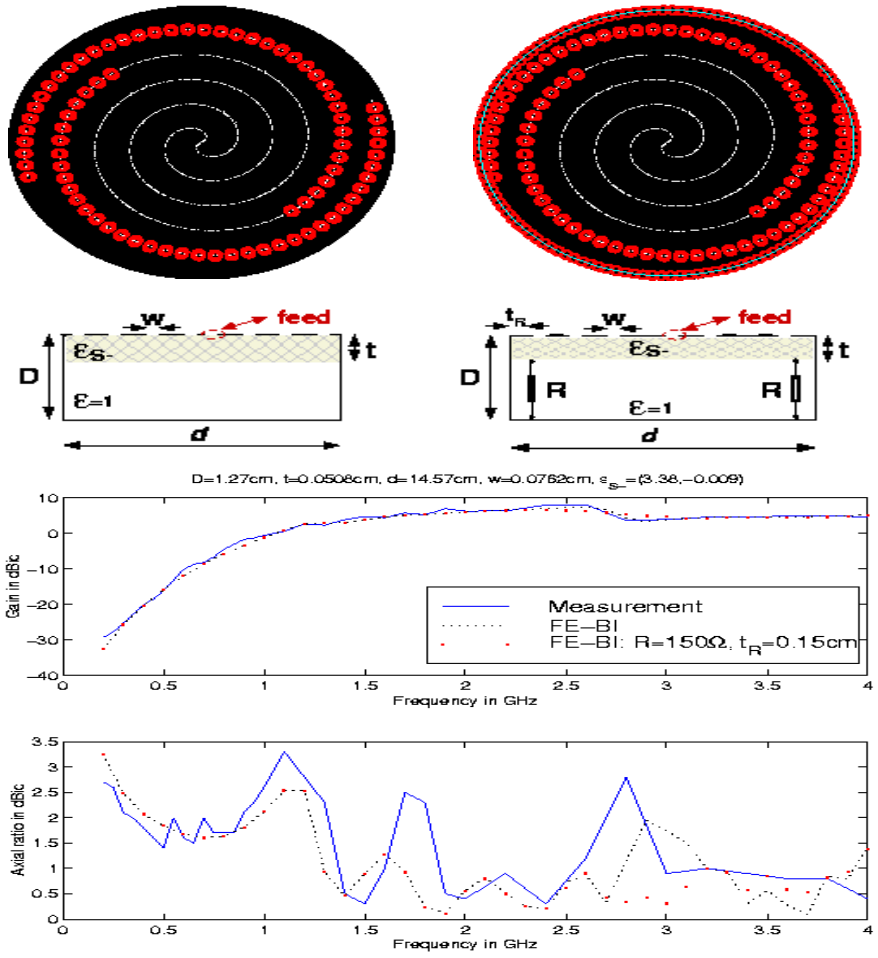

Figure 3. Geometry and performance of the broadband slot spiral for personal communications (simulation used 10,300 prisms which resulted in 23561 unknowns of which 773 were boundary integral unknowns); See M.W. Nurnberger and J.L. Volakis (1999 IEEE Antenna Propag. Symposium, Orlando, FL., USA) for more details on the slot spiral antenna.